



Title	Size and structure-dependent photocatalytic activity of jingle-bell-shaped silica-coated cadmium sulfide nanoparticles for methanol dehydrogenation
Author(s)	Pal, Bonamali; Torimoto, Tsukasa; Iwasaki, Kentaro; Shibayama, Tamaki; Takahashi, Heishichiro; Ohtani, Bunsho
Citation	Journal of physical chemistry. B, 108(48), 18670-18674 <a href="https://doi.org/10.1021/jp046445h">https://doi.org/10.1021/jp046445h</a>
Issue Date	2004-12-02
Doc URL	<a href="http://hdl.handle.net/2115/52786">http://hdl.handle.net/2115/52786</a>
Type	article
File Information	jp046445h.pdf



[Instructions for use](#)

# Size and Structure-Dependent Photocatalytic Activity of Jingle-Bell-Shaped Silica-Coated Cadmium Sulfide Nanoparticles for Methanol Dehydrogenation

Bonamali Pal,<sup>†</sup> Tsukasa Torimoto,<sup>†,‡,§</sup> Kentaro Iwasaki,<sup>§</sup> Tamaki Shibayama,<sup>||</sup> Heishichiro Takahashi,<sup>||</sup> and Bunsho Ohtani<sup>\*,†,§</sup>

“Light and Control”, PRESTO, Japan Science and Technology Agency, 4-1-8 Honcho Kawaguchi, Saitama 332-0012, Japan, Catalysis Research Center, Hokkaido University, Sapporo 001-0021, Japan, Graduate School of Environmental Earth Science, Hokkaido University, Sapporo 060-0811, Japan, and Center for Advanced Research of Energy Technology, Hokkaido University, Sapporo 060-8628, Japan

Received: August 6, 2004; In Final Form: September 22, 2004

Silica-coated cadmium sulfide nanoparticles ( $\text{SiO}_2/\text{CdS}$ ) having a jingle-bell structure were prepared via size-selective photoetching and were used as photocatalysts for dehydrogenation of methanol. Irradiation of  $\text{SiO}_2/\text{CdS}$  suspended in an aqueous solution containing methanol induced the liberation of hydrogen ( $\text{H}_2$ ), the amount of which increased linearly with increase in the time of irradiation. The observed stable photocatalytic activity was attributed to the prevention of coalescence between CdS core particles by the surrounding  $\text{SiO}_2$  shells during the photocatalytic reaction. The rate of  $\text{H}_2$  liberation increased with decrease in the wavelength of irradiation light for the size-selective photoetching, that is, the smaller the size of the CdS core, the higher the rate of  $\text{H}_2$  liberation, probably because of increased reduction and oxidation abilities of CdS as a result of decrease in their particle size, that is, size quantization effect. Rhodium photodeposited on  $\text{SiO}_2/\text{CdS}$  worked as a cocatalyst for the enhancement of dehydrogenation. The photocatalytic activity was reduced by increase in shell thickness because of a decrease in the rate of penetration of chemical species or the transfer of electrons and holes through the  $\text{SiO}_2$  layer. Also, the close contact between the core and shell retarded the photocatalytic reaction, indicating that the surface of the CdS core for methanol dehydrogenation was covered with a  $\text{SiO}_2$  shell layer. The results indicate that the jingle-bell-shaped  $\text{SiO}_2/\text{CdS}$  nanoparticles can be an efficient and stable photocatalyst with a flexibly tunable structure, in contrast to surface-modified CdS particles prepared by a conventional technique.

## Introduction

Photoexcitation of a valence-band (VB) electron into a conduction band (CB) leaving a positive hole in VB is the primary process of photocatalytic reaction. The photoexcited electron and positive hole undergo relaxation to the bottom of the CB and top of the VB, respectively, and induce reduction and oxidation of chemical substances adsorbed on the surface of the photocatalyst.<sup>1–4</sup> Although little experimental evidence has been obtained for particulate photocatalysts, it is believed that the position of CB and VB edges determine the reduction and oxidation abilities, respectively, of the photocatalysts. The position is assumed to be the same when a given crystal of a semiconducting material is used as a photocatalyst unless the size of crystallite is small as described below. It has been reported that the different VB positions between titanium oxide ( $\text{TiO}_2$ ) and cadmium sulfide (CdS) can explain the difference in product selectivity for the photocatalytic reactions by their suspensions.<sup>5</sup> On the other hand, the CB and VB positions of given crystallites vary depending on the size of particles if the

size is small enough, for example, in the range of few nanometers, to induce a size quantization effect; the smaller the size is, the higher and lower are the positions of CB and VB, respectively, and hence the larger is the energy gap between the CB and VB.<sup>6–9</sup> It would therefore be possible to control the redox ability of photocatalyst nanoparticles by changing their size. However, there are two reasons to disturb realization of this control. One is difficulty in stabilization of such small particles since they tend to aggregate into large ones. The other is difficulty in preparation of small particles of monodispersed size; the use of conventional procedures often gives a relatively large size distribution, which obscures the size-dependent photocatalytic activity or reaction selectivity.

We have reported<sup>10,11</sup> a novel synthesis of silica ( $\text{SiO}_2$ )-coated CdS ( $\text{SiO}_2/\text{CdS}$ ) with a void space, jingle-bell-shaped nanocomposites, in which a CdS core was incorporated in hollow  $\text{SiO}_2$  shell particles, using a size-selective photoetching technique. The size of the CdS core can be adjusted from 3.7 to 2.8 nm with relatively narrow size distributions by using monochromatic light with a wavelength of 514–458 nm. It has also been proved that the  $\text{SiO}_2$  shells are thin enough to allow penetration of molecules and ions through them, and this enables the CdS cores to act as a photocatalyst without their coalescence.<sup>12</sup> We report here the results of photocatalytic methanol dehydrogenation using jingle-bell-shaped  $\text{SiO}_2/\text{CdS}$  particles of different core sizes and we discuss the influence of their nanostructure, for example, core size, loaded rhodium (Rh) metal

\* Author to whom correspondence should be addressed. E-mail: ohtani@cat.hokudai.ac.jp; address: Catalysis Research Center, Hokkaido University, Sapporo 001-0021, Japan; phone: +81-11-706-9132; fax: +81-11-706-9133.

<sup>†</sup> Japan Science and Technology Agency.

<sup>‡</sup> Catalysis Research Center, Hokkaido University.

<sup>§</sup> Graduate School of Environmental Earth Science, Hokkaido University.

<sup>||</sup> Center for Advanced Research of Energy Technology, Hokkaido University.

deposits, and shell thickness, on the photocatalytic activity to show the superiority of the jingle-bell-shaped nanoparticles.

### Experimental Section

**Materials.** Sodium bis(2-ethylhexyl)sulfosuccinate (AOT), 1,1'-dimethyl-4,4'-bipyridinium dichloride (methyl viologen, MV<sup>2+</sup>), and 3-mercaptopropyltrimethoxysilane (MPTS) were purchased from Tokyo Chemical Industry. Cadmium perchlorate (Kishida Reagents Chemicals) was used as received. Other chemicals used in this study were supplied from Wako Pure Chemical Industries. Aqueous solutions were prepared just before use with water purified by a Yamato/Millipore WP501 Milli-Q system.

**Preparation of Silica-Coated Cadmium Sulfide (SiO<sub>2</sub>/CdS) Nanoparticles.** SiO<sub>2</sub>/CdS having a thin shell layer (SiO<sub>2</sub>(thin)/CdS) was synthesized through modification of CdS particle surface with 3-mercaptopropyltrimethoxysilane (MPTS) followed by hydrolysis of its trimethoxysilyl group, as reported in our previous papers.<sup>10</sup> The starting bare CdS nanoparticles having an average diameter of 5.0 nm were prepared by an AOT-reversed-micelle method with a concentration ratio,  $w$  ( $=[\text{H}_2\text{O}]/[\text{AOT}]$ ), of 12. The shell thickness was increased, if necessary, by hydrolysis of tetraethyl orthosilicate (TEOS) in the presence of MPTS-modified CdS nanoparticles (the details of the preparation procedure will be published elsewhere),<sup>13</sup> and the obtained powder was labeled SiO<sub>2</sub>(thick)/CdS. The thicknesses of the SiO<sub>2</sub> shell layers of SiO<sub>2</sub>(thin)/CdS and SiO<sub>2</sub>(thick)/CdS were estimated to be ca. 0.3 and 0.9 nm, respectively,<sup>13</sup> by using the total amount of silicon and oxygen atoms in SiO<sub>2</sub> shell determined from the results of elemental analyses of particles assuming that a SiO<sub>2</sub> layer uniformly covered the surface of CdS core with a diameter of 5.0 nm.

These SiO<sub>2</sub>/CdS powders were subjected to size-selective photoetching using an argon ion laser with wavelengths of 514, 488, and 458 nm. The average size ( $d_{\text{av}}$ ) of original CdS nanoparticles (5.0 nm) became small with decrease in wavelength of the monochromatic laser light. CdS nanoparticles photoetched at 514 and 458 nm were shown in a previous study to have  $d_{\text{av}}$  of 3.7 and 2.8 nm, respectively,<sup>10</sup> and  $d_{\text{av}}$  of CdS photoetched at 488 nm was determined to be 3.4 nm in this study by using a JEOL 2010F transmission electron microscope (TEM) with an acceleration voltage of 200 kV. For comparison, original SiO<sub>2</sub>(thin)/CdS particles having smaller CdS core size were prepared in AOT reversed micelles of smaller size ( $w = 6.3$ ) and were covered with SiO<sub>2</sub> shells in a similar way. The CdS core size of thus-obtained core-shell particles was estimated to be 2.4 nm from the exciton peak position at 424 nm on the basis of a theoretical relation between energy gap and particle diameter of CdS.<sup>14</sup> These particles were used without photoetching.

**Preparation of 2-Mercaptoethanol-Modified CdS Nanoparticles (RSH/CdS).** Conventional surface modification was also applied to stabilize CdS nanoparticles photoetched by 458-nm irradiation. Bare CdS nanoparticles ( $d_{\text{av}} = 5.0$  nm) (0.17 mmol) were subjected to size-selective photoetching in toluene solution (72 cm<sup>3</sup>) containing AOT (5.7 g), water (0.7 cm<sup>3</sup>), and methyl viologen (0.7 μmol). After the absorption spectrum of the solution became almost unchanged, 2-mercaptoethanol (0.13 mmol) was added to modify the surfaces of the photoetched CdS particles, followed by stirring overnight. Then, methanol was added to destroy the reverse micelles, resulting in the precipitation of 2-mercaptoethanol-modified CdS nanoparticles (RSH/CdS). The powder was washed with methanol several times and dried under vacuum. Since the size of CdS nanopar-

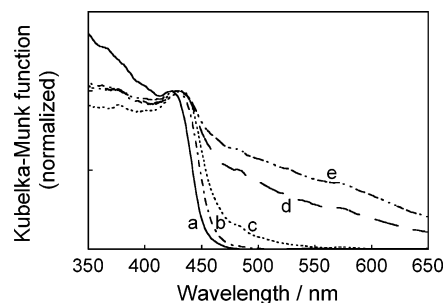


**Figure 1.** Diffuse reflectance spectra of SiO<sub>2</sub>/CdS photoetched at 458 nm (a) and those after Rh deposition with amounts of 0.37 (b), 1.9 (c), 5.7 (d), and 11 at. % (e).

ticles was simply controlled by choosing the wavelength of irradiation light, irrespective of the kind of the stabilizers used in the preparation of CdS nanoparticles,<sup>15,16</sup> the CdS size of RSH/CdS was assumed to be the same as that of SiO<sub>2</sub>/CdS photoetched at 458 nm, that is, 2.8 nm.

**Photocatalytic Deposition of Rhodium on the Photocatalyst Particles.** Deposition of rhodium (Rh) onto SiO<sub>2</sub>/CdS or RSH/CdS was carried out through photocatalytic reduction of rhodium(III) ion (Rh<sup>3+</sup>) by CdS particles themselves as a photocatalyst.<sup>17</sup> Each powder (12 mg) was suspended in an aqueous solution (5 cm<sup>3</sup>) containing methanol (50 vol %) and rhodium(III) chloride (RhCl<sub>3</sub>·3H<sub>2</sub>O) and then irradiated with a 400-W high-pressure mercury lamp ( $\lambda > 300$  nm) for 1.5 h under an argon atmosphere, followed by centrifugation, washing with water several times, and drying under vacuum. The amount of Rh loading ranged from 0.09 to 19 at. % based on that of Cd atoms in the powders. For the measurement of diffuse reflectance spectra, sample powders were diluted with a powder of barium sulfate to give a content of 1 wt % and were measured in a dry state using a photonic multichannel analyzer (Hamamatsu Photonics, PMA-11) and pure barium sulfate as a reference.

**Preparation of Platinum Colloidal Particles.** A black-colored platinum (Pt) sol was prepared following the reported procedure.<sup>18,19</sup> An aqueous solution (150 cm<sup>3</sup>) containing chloroplatinic acid (H<sub>2</sub>PtCl<sub>6</sub>·6H<sub>2</sub>O) (30 mg) and sodium citrate (0.30 g) was refluxed for 4 h. After cooling, the sol was treated with an Amberlite MB-3 ion-exchange resin to remove excess citrate and inorganic electrolytes and was filtered. The average size of Pt particles was determined to be about 60 nm by a scanning tunneling microscope (Molecular Imaging, PicoSPM).

**Photocatalytic Methanol Dehydrogenation.** Photocatalytic methanol dehydrogenation was performed by monochromatic irradiation at 436 nm that was extracted from a high-pressure mercury lamp (Eiko-sha, 400 W) using glass filters (Asahi Techno Glass, V-42 and Y-43). The irradiation intensity was 7.3 mW cm<sup>-2</sup>. Each photocatalyst containing 6 mg CdS was suspended in an aqueous solution (5.0 cm<sup>3</sup>) containing methanol (50 vol %) and irradiated under an argon atmosphere at 298 K with vigorous magnetic stirring (ca. 1000 rpm). The colloidal Pt particles were added to the reaction suspension to give 0.24 at. %, when necessary. The amount of liberated hydrogen (H<sub>2</sub>) was measured with a gas chromatograph (Shimadzu GC 8A) equipped with a molecular sieve 5A column and a thermal conductivity detector (TCD) using argon as a carrier.

### Results and Discussion

Figure 1 shows diffuse reflectance spectra of 458-nm-photoetched SiO<sub>2</sub>(thin)/CdS particles and those of particles loaded with various amounts of Rh. With the increase in Rh

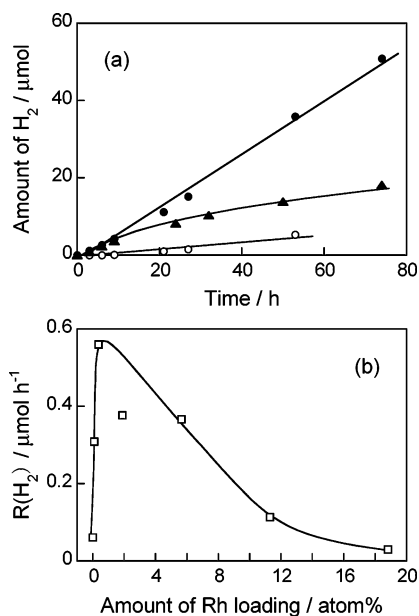


**Figure 2.** (a) Time courses of hydrogen liberation by various photocatalysts. Photocatalysts used were 458-nm-photoetched SiO<sub>2</sub>/CdS with (solid circles) and without (open circles) Rh loading, and Rh-loaded RSH/CdS photoetched at 458 nm (triangles). The amount of Rh loading was 0.37 at. %. (b) Relationship between hydrogen evolution rate ( $R(H_2)$ ) and amount of Rh loaded on 458-nm-photoetched SiO<sub>2</sub>/CdS.

loading, an absorption band assigned to Rh metal nanoparticles<sup>20</sup> developed in the range of wavelengths larger than 470 nm. On the other hand, a peak observed at ca. 425 nm, which appeared after the size-selective photoetching at 458 nm and was assigned to an exciton of CdS, was slightly red-shifted to ca. 431 nm by the photodeposition of Rh, irrespective of the amount of deposition. When the energy gap of CdS nanoparticles was estimated from the exciton peak position and fitted to a theoretical relation between energy gap and particle diameter of CdS,<sup>14</sup> the diameter of 458-nm-photoetched CdS core and that with Rh loading were estimated to be 2.5 and 2.6 nm, respectively, indicating negligible change in CdS core size by Rh photodeposition. The 458-nm-photoetched SiO<sub>2</sub>(thin)/CdS particles had a jingle-bell structure, as reported in our previous paper,<sup>10</sup> and the photodeposition of Rh might occur on the surfaces of CdS nanoparticles, that is, Rh nanoparticles are deposited in the void space of SiO<sub>2</sub>/CdS. On the other hand, irradiation of the original SiO<sub>2</sub>(thin)/CdS in the presence of Rh<sup>3+</sup> also exhibited the development of a similar broad absorption band at wavelengths longer than 500 nm despite the absence of void spaces in their particles. This fact suggested that SiO<sub>2</sub>(thin)/CdS prepared in this study had a shell that was thin enough to allow the photodeposition of Rh on the outer surface of the SiO<sub>2</sub> shell and to allow electron and hole transfer through it. Therefore, we could not rule out the possibility that Rh nanoparticles were photodeposited on the outer surface of the SiO<sub>2</sub> shell as well as in the void space of SiO<sub>2</sub>/CdS when 458-nm-photoetched SiO<sub>2</sub>(thin)/CdS was used as a starting material.

Figure 2a shows the time course of H<sub>2</sub> liberation from the suspensions of SiO<sub>2</sub>(thin)/CdS with and without Rh loading. SiO<sub>2</sub>(thin)/CdS photoetched at 458 nm showed an almost linear increase in the amount of H<sub>2</sub> both in the presence and absence of Rh, while the Rh loading considerably accelerated the dehydrogenation. By irradiation of 458-nm-photoetched SiO<sub>2</sub>/CdS with Rh loading for 70 h, the H<sub>2</sub> yield exceeded 50 μmol, 1.2-times greater than the total molar amount of CdS. Furthermore, the diffuse reflectance spectrum of 458-nm-photoetched

SiO<sub>2</sub>(thin)/CdS particles was almost unchanged during the photocatalytic reaction. These results indicated that the methanol dehydrogenation proceeds photocatalytically and that Rh particles act as a cocatalyst for the effective reduction of protons (H<sup>+</sup>) with photogenerated electrons in CdS, as reported by Fendler and co-workers.<sup>17</sup>

On the other hand, when RSH/CdS nanoparticles prepared by photoetching at 458 nm were used as a photocatalyst, the time-course curve was not linear: at the early stage of irradiation (<10 h), Rh-loaded RSH/CdS exhibited a rate of H<sub>2</sub> liberation similar to that of Rh-loaded SiO<sub>2</sub>(thin)/CdS, but the rate was decreased by prolonged irradiation. The exciton peak of RSH/CdS nanoparticles in diffuse reflectance spectra was red-shifted from 438 to 454 nm after irradiation for 70 h, indicating that RSH/CdS coalesced into larger particles, being different from the behavior of 458-nm-photoetched SiO<sub>2</sub>(thin)/CdS described above. These observations can be explained by the structural difference in the photocatalysts. In SiO<sub>2</sub>(thin)/CdS, the surrounding SiO<sub>2</sub> shell is stable enough to prevent coalescence between CdS nanoparticles during the photocatalytic reaction, but the irradiation of RSH/CdS possibly caused partial detachment of 2-mercaptoethanol from the CdS core surface by oxidation with photogenerated holes, resulting in the coalescence of CdS nanoparticles. The increase in the CdS size caused a reduction in the level of the photocatalytic activity of nanoparticles, as described below.

From the slope of the linear time-course curve of H<sub>2</sub> liberation, the rate of dehydrogenation,  $R(H_2)$ , was calculated. Figure 2b shows the dependence of  $R(H_2)$  on the amount of Rh loading on 458-nm-photoetched SiO<sub>2</sub>(thin)/CdS. As the amount of Rh increased,  $R(H_2)$  increased up to an optimum at 0.37 at. % Rh loading, owing to the increase in the number of catalytic sites for H<sub>2</sub> liberation, while further loading resulted in a gradual decrease in  $R(H_2)$ . The excessive Rh loading possibly covers the CdS surface to obstruct photoabsorption by the CdS cores and to enhance recombination of photogenerated electrons and holes, resulting in a decrease in the photocatalytic activity of CdS nanoparticles. Similar behavior has been observed for H<sub>2</sub> liberation induced by Pt-loaded TiO<sub>2</sub> photocatalysts.<sup>21</sup>

Rates of dehydrogenation for several CdS photocatalysts are summarized in Table 1. In all cases, Rh loading enhanced the photocatalytic activity, and the degree of enhancement varied depending on the kind of photocatalyst. To discuss the photocatalytic activity, we presumed that four significant parameters, size of the CdS core particles, thickness of the SiO<sub>2</sub> shell layer, size of the void space, and distribution of loaded Rh deposits, should be taken into account. First, the photocatalytic activity of SiO<sub>2</sub>/CdS nanoparticles without void spaces (entries 2 and 7) is compared with that of commercial crystalline CdS (entry 1). When the particles were loaded with Rh on their outermost surface, that is, SiO<sub>2</sub>, Rh deposits catalyzed H<sub>2</sub> liberation and the activity increased with decrease in CdS (core) size. Since the molar ratio of Rh/CdS was constant, that is, no significant variation of the number of H<sub>2</sub> liberation sites may be expected for all of the photocatalysts shown in Table 1, an increase in the specific surface area of CdS particles caused by the decrease in their particle size does not seem to be a predominant reason for this behavior; stronger redox properties of the smaller CdS may also account for the behavior. In the absence of loaded Rh, a similar tendency was observed, but the original SiO<sub>2</sub>/CdS (entry 2) gave a smaller rate presumably because of the coverage of the CdS surface with SiO<sub>2</sub>.

A comparison of the activities of photocatalysts (entries 3–5) prepared by photoetching of the original SiO<sub>2</sub>/CdS (entry 2)

**TABLE 1: Rate of H<sub>2</sub> Liberation (R(H<sub>2</sub>)) Observed for CdS Photocatalysts**

entry	sample	$\lambda_{\text{photoetch}}/\text{nm}^a$	CdS size/nm	shell thickness/nm	void space/nm	R(H <sub>2</sub> )/nmol h <sup>-1b</sup>		
						as-prepared	with Rh <sup>c</sup>	with Pt <sup>d</sup>
1	bulk CdS (Furuuchi)	none	> 100	0	0	1.9	4.5	16
2	SiO <sub>2</sub> (thin)/CdS ( <i>w</i> = 12)	none	5.0	0.3	0	0.88	86	1.3
3	SiO <sub>2</sub> (thin)/CdS ( <i>w</i> = 12)	514	3.7	0.3	1.4	4.7	61	
4	SiO <sub>2</sub> (thin)/CdS ( <i>w</i> = 12)	488	3.4	0.3	1.6	4.5	150	
5	SiO <sub>2</sub> (thin)/CdS ( <i>w</i> = 12)	458	2.8	0.3	2.4	60	560	70
6	SiO <sub>2</sub> (thick)/CdS ( <i>w</i> = 12)	458	2.8	0.9	2.4	0.34	2.3	
7	SiO <sub>2</sub> (thin)/CdS ( <i>w</i> = 6.3)	none	2.4 <sup>e</sup>	0.3 <sup>f</sup>	0	40	260	

<sup>a</sup> Wavelength of the monochromatic light used for the size-selective photoetching. <sup>b</sup> Obtained by using photocatalysts containing 6 mg CdS suspended in methanol–water (1:1) solutions. <sup>c</sup> Amount of photodeposited Rh was 0.37 at. %. <sup>d</sup> Colloidal Pt particles were added to give 0.24 at. %. <sup>e</sup> Estimated from the exciton peak position according to a theoretical relation between the energy gap and particle diameter of CdS. <sup>f</sup> Estimated by analogy with that of particles of entry 2.

showed that an increase in activity with decrease in core size occurred both in the presence and absence of loaded Rh in all cases, except for the case of a photocatalyst prepared by photoetching at 514 nm, which exhibited activity lower than that of larger particles (entry 2) in the presence of Rh and almost the same as or even higher than that of smaller particles (entry 4) in the absence of Rh. This exception may have been caused by nonuniform photoetching and Rh deposition; since the original particles have a size distribution ranging from 3.3 to 6.9 nm and since 514-nm irradiation results in the formation of a CdS core with an average size of 3.7 nm, only some of the CdS particles might have been photoetched to smaller ones, resulting in the production of a mixture of core–shell particles with and without void spaces. One possibility is that Rh deposition proceeded preferably on the nonetched particles rather than in the inner space, and thereby only some of the SiO<sub>2</sub>/CdS particles were activated. Similar enhancement of photocatalytic activity with a decrease in the size of semiconductor nanoparticles has been reported for several kinds of photocatalytic reactions, such as the production of hydrogen peroxide<sup>22</sup> and the photoreduction of carbon dioxide,<sup>23</sup> nitrate,<sup>24</sup> and methyl viologen.<sup>25</sup> Recently, we have experimentally clarified that the decrease in the size of size-quantized CdS nanoparticles induces a negative shift in the potential of the conduction band edge of CdS particles as well as a positive shift in that of the valence band edge.<sup>26</sup> Since the size of the CdS core became smaller with a decrease in the light wavelength for the photoetching, the decrease in CdS core size could enlarge the overpotentials both of H<sup>+</sup> reduction with photogenerated electrons and of methanol oxidation with positive holes to induce higher photocatalytic activity.

The fact that solid SiO<sub>2</sub>/CdS particles whose CdS-core size was small enough (entry 7) showed activity lower than that of the corresponding jingle-bell-shaped particles (entry 5) suggests the importance of not only core size but also void space between the core and shell. Another factor worth noting is thickness of the SiO<sub>2</sub> shell. The 458-nm photoetched SiO<sub>2</sub>(thick)/CdS (entry 6) exhibited much smaller R(H<sub>2</sub>) than that obtained with SiO<sub>2</sub>(thin)/CdS (entry 5) even when Rh was photodeposited. As reported in our previous papers,<sup>10</sup> thin SiO<sub>2</sub> shell layer (ca. 0.3-nm thickness) had small pores and some chemical species could penetrate inside the void space from the bulk solution. Therefore, these results suggested that the increase in the thickness of SiO<sub>2</sub> layer prevented the permeation of the reaction substrate, methanol, probably because of the removal of small pores presented in thin SiO<sub>2</sub> shell and/or decreased the tunneling probabilities of electron/hole transfer through an SiO<sub>2</sub> layer.

It is well-known that Pt nanoparticles effectively scavenge the photogenerated electrons in semiconductor particles and work as cocatalysts for H<sub>2</sub> liberation.<sup>3,21</sup> In the present study,

the addition of colloidal Pt particles to the bulk CdS particles enhanced the H<sub>2</sub> evolution rate (entry 1) ca. 8 times, the degree of which was larger than that of Rh deposits probably because of the difference in the catalytic activity of metal surface for H<sub>2</sub> liberation. In the SiO<sub>2</sub>/CdS particles (entries 2 and 5), however, photocatalytic activity was little improved by the addition of Pt particles, irrespective of the photoetching of CdS core, while the photodeposited Rh induced the large enhancement as mentioned above. These results indicated that the SiO<sub>2</sub> shell prevented the contact between the surfaces of CdS and Pt probably because the shell had no pore large enough for Pt particles having the diameter of ca. 60 nm to enter; so, the probability of electron transfer from the photoexcited CdS to Pt particles remarkably declined, though the SiO<sub>2</sub> shell had small pores through which ionic species such as Cd<sup>2+</sup> and SO<sub>4</sub><sup>2-</sup> were passed as reported in our previous paper.<sup>10</sup> Consequently it was suggested that the photodeposition of Rh on SiO<sub>2</sub>/CdS made the electronic contact between CdS cores and Rh particles and then the photogenerated electrons in CdS were effectively scavenged by the loaded metal particles, even if Rh particles were photodeposited on the outer surface of the shell of the original SiO<sub>2</sub>/CdS, where the electronic contact might be attained through the metal photodeposited inside the small pores of SiO<sub>2</sub> shell.

## Conclusions

This work has demonstrated the advantage of SiO<sub>2</sub>/CdS nanocomposites having a jingle-bell structure as photocatalysts. Size-selective photoetching of SiO<sub>2</sub>/CdS and the following photodeposition of cocatalysts on the CdS core enabled optimization of photocatalytic activity. The SiO<sub>2</sub> shell structure was maintained during the photocatalytic reaction and prevented coalescence between CdS cores, resulting in superior stability of SiO<sub>2</sub>/CdS compared to that of CdS nanoparticles prepared by conventional surface modification methods. Furthermore, the photocatalytic activity of SiO<sub>2</sub>/CdS can be tuned by changing both the size of the CdS core and the nanostructure of core–shell particles, where the void space inside the SiO<sub>2</sub> shell worked as a space for photocatalytic reaction. Therefore, jingle-bell-shaped size-quantized semiconductor core–SiO<sub>2</sub> shell particles are promising for both the investigation of chemical events on a nanoparticle surface and their control, which have never been attained because of the instability of nanoparticles prepared by conventional methods. Study along this line is currently in progress.

**Acknowledgment.** This research was partially supported by a Grant-in-Aid for Scientific Research (B) (No. 16350095) from the Japan Society for the Promotion of Science.

## References and Notes

- (1) Hoffmann, M. R.; Martin, S. T.; Choi, W.; Bahnemann, D. W. *Chem. Rev.* **1995**, *95*, 69–96.
- (2) Nozik, A. J.; Memming, R. *J. Phys. Chem.* **1996**, *100*, 13061–13078.
- (3) Mills, A.; Sawunyama, P. *J. Photochem. Photobiol., A* **1997**, *108*, 1–35.
- (4) Kamat, P. V.; Meisel, D. *Curr. Opin. Colloid Interface Sci.* **2002**, *7*, 282–287.
- (5) Ohtani, B.; Yako, T.; Samukawa, Y.; Nishimoto, S. I.; Kanamura, K. *Chem. Lett.* **1997**, 91–92.
- (6) Steigerwald, M. L.; Brus, L. E. *Annu. Rev. Mater. Sci.* **1989**, *19*, 471–495.
- (7) Weller, H. *Angew. Chem., Int. Ed. Engl.* **1993**, *32*, 41–53.
- (8) Murray, C. B.; Kagan, C. R.; Bawendi, M. G. *Annu. Rev. Mater. Sci.* **2000**, *30*, 545–610.
- (9) Parak, W. J.; Manna, L.; Simmel, F. C.; Gerion, D.; Alivisatos, P. In *Nanoparticles*; Schmid, G., Ed.; Wiley-VCH Verlag GmbH & Co. KGaA: Weinheim, Germany, 2004; pp 4–49.
- (10) Torimoto, T.; Reyes, J. P.; Iwasaki, K.; Pal, B.; Shibayama, T.; Sugawara, K.; Takahashi, H.; Ohtani, B. *J. Am. Chem. Soc.* **2003**, *125*, 316–317.
- (11) Torimoto, T.; Reyes, J. P.; Murakami, S. Y.; Pal, B.; Ohtani, B. *J. Photochem. Photobiol., A* **2003**, *160*, 69–76.
- (12) Iwasaki, K.; Torimoto, T.; Shibayama, T.; Takahashi, H.; Ohtani, B. *J. Phys. Chem. B* **2004**, *108*, 11946–11952.
- (13) Pal, B.; Torimoto, T.; Ikeda, S.; Shibayama, T.; Sugawara, K.; Takahashi, H.; Ohtani, B. *Top. Catal.*, accepted for publication.
- (14) Nosaka, Y. *J. Phys. Chem.* **1991**, *95*, 5054–5058.
- (15) Torimoto, T.; Kontani, H.; Sakata, T.; Mori, H.; Yoneyama, H. *Chem. Lett.* **1999**, 379–380.
- (16) Torimoto, T.; Kontani, H.; Shibutani, Y.; Kuwabata, S.; Sakata, T.; Mori, H.; Yoneyama, H. *J. Phys. Chem. B* **2001**, *105*, 6838–6845.
- (17) Tricot, Y. M.; Fendler, J. H. *J. Am. Chem. Soc.* **1984**, *106*, 7359–7366.
- (18) Turkevich, J.; Kim, G. *Science* **1970**, *169*, 873.
- (19) Ohtani, B.; Aoki, E.; Iwai, K.; Nishimoto, J. *Photosci.* **1994**, *1*, 31–37.
- (20) Creighton, J. A.; Eadon, D. G. *J. Chem. Soc., Faraday Trans.* **1991**, *87*, 3881–3891.
- (21) Ohtani, B.; Iwai, K.; Nishimoto, S.-i.; Sato, S. *J. Phys. Chem. B* **1997**, *101*, 3349–3359.
- (22) Hoffman, A. J.; Carraway, E. R.; Hoffmann, M. R. *Environ. Sci. Technol.* **1994**, *28*, 776–785.
- (23) Inoue, H.; Torimoto, T.; Sakata, T.; Mori, H.; Yoneyama, H. *Chem. Lett.* **1990**, 1483–1486.
- (24) Korgel, B. A.; Monbouquette, H. G. *J. Phys. Chem. B* **1997**, *101*, 5010–5017.
- (25) Matsumoto, H.; Uchida, H.; Matsunaga, T.; Tanaka, K.; Sakata, T.; Mori, H.; Yoneyama, H. *J. Phys. Chem.* **1994**, *98*, 11549–11556.
- (26) Miyake, M.; Torimoto, T.; Sakata, T.; Mori, H.; Yoneyama, H. *Langmuir* **1999**, *15*, 1503–1507.